VISUALISATION OF MICRO FRACTURE NETWORK IN AN OILWET CARBONATE

Wim Looyestijn, Arjen Cense, Jan Hofman, Fons Marcelis and Axel Makurat
Shell International Exploration and Production B.V., Rijswijk, The Netherlands

This paper was prepared for presentation at the International Symposium of the Society of Core Analysts held in Noordwijk, The Netherlands 27-30 September, 2009

ABSTRACT

Waterflooding in an oilwet carbonate can easily be jeopardized by the presence of fractures, even if they have widths in the micrometer range. Such dimensions are far below the traditional resolution of CT scanners used for monitoring flooding experiments on whole cores, and thus can be overlooked during the interpretation and sub-sequent up-scaling of laboratory results. The experiments shown here were made on preserved whole cores, taken from a carbonate reservoir that is known to be very oilwet. The cores were mounted in a CT-transparent coreholder and scanned in full 3D using a medical scanner continuously during the flooding experiments. We applied a combination of two techniques to make the fracture network visible, and to determine the fracture width quantitatively. The first technique is the well-known method to enhance the X-ray attenuation of one of the fluid by adding a suitable substance. In this case, once the water flood had become stable, we replace the NaCl brine by a mole-equivalent NaI brine. Subtracting CT-scans, taken subsequently with each brine, revealed that water had not been replaced in the matrix, and only through a fine fracture network through the core. No leakage was observed along the outside of the core. The second technique is a two-step deconvolution, to first remove the smoothing caused by the inversion kernel of the CT-scanner, and second to interpret the observed value in terms of a fraction of the pixel dimension. The thus found range of fracture widths agrees well with the analytical estimation of fracture width estimated from fluid low and pressure drop.

INTRODUCTION

The purpose of the project was to run a waterflood test on a whole core piece taken from a bioturbated interval in an oilwet carbonate reservoir. Dynamic properties are normally determined on 2.5 or 4 cm diameter samples, which are too small to capture the effects of heterogeneity features ("nodules") that are of the same size as these samples. The project aims at monitoring the saturation change during the water flood in a CT scanner [1]. The results would then serve as an experimental verification of a numerical simulation that would be based on a CT-derived porosity map and separate dynamic properties for the nodules and matrix material. The discovery of an unexpected fracture prompted us to a modification of the experiment with the aim to characterize this fracture.

A preserved core piece of approximately 10 cm diameter and 30 cm length was selected. Initial scans show the presence of nodules throughout the sample and no clear fractures apart from a few very localized short fractures. The core was used in fresh state.

EXPERIMENTAL PROCEDURE

Core Holder

Contrary to plug samples that can be made to a specific size, each whole core is different in length and diameter. As a consequence, the core holder has to be made to size for each core separately. A further complication for the present project is that the core holder has to be CT-transparent, which excludes the normal designs employing a steel housing. Because of the relatively low demands on fluid pressure and temperature in this experiment, it was decided to mount the core in an aluminium tube and to fill the ~ 4 - 6 mm annulus with a CT-transparent epoxy resin. The resin was to seal off the surface of the core and fill the local irregularities (which would be difficult to do with a sleeve). The tube is fitted with end flanges containing radial and cylindrical grooves for even distribution and gathering of the fluids over the end faces. The aluminium tube and end flanges have separate heaters to keep the assembly at the selected temperature while fluids are flooded; the low flow rates are slow enough to ensure that the fluids have warmed up before entering the core. The core holder is placed inside a Perspex cage in which hot air from the heaters is homogeneously distributed by a fan. No back pressure was used.

Differential pressures were taken from the flow lines at either side of the core, and absolute pressure at the inflow side. Three temperature sensors (thin thermocouple wires) were mounted at approximately ¼, ½ and ¾ of the core length. The wire was lead along the core, i.e. in the annular space, to feed-throughs in the end flange.

Water and oil floods

To remove the gas, the preserved core was first flooded with (dead) oil. For this process, the core was put in a vertical position and the temperature was raised to 40^{o}C. After an additional throughput of 250 cm^3 of oil, the core was put in a horizontal position and oil flow continued for the oil permeability measurement. During this process, no water was expelled, confirming that there was no moveable water present. From the injection flow rate and pressure differential we compute a $K_{o,wc}$ of 47 mD.

We started the waterflood by flowing formation water at a rate of 0.4 cm^3/min, roughly equivalent to 1 ft/d. The core was CT-scanned in 3D at one-hour intervals. After an initial oil production of only 15 cm^3 (equals 0.03 pore volume), water break-through was observed. The pressure stabilised, corresponding to a water permeability of about 15 mD. Injection was continued for 24 hours without any further oil production.

Inspection of differential CT scans was made on-line to spot locations where changes in saturation had occurred, or, as suspected, the water had found a by-pass. However, the scans did not reveal where the water was flowing. This is not surprising as the equivalent permeability of 15 mD does not require a big pass way.
To enhance the visibility of the water, we replaced the formation water NaCl by NaI brine which has a rather strong absorption to X-rays; see, for example [2]. After 28 hrs of injecting formation water (~100 kppm NaCl equivalent) we injected NaI brine (equivalent mole concentration) for 3½ hrs (~85 cm^3 ≅ 0.15 PV); thereafter we continued with the formation water for another 18 hrs (~400 cm^3 ≅ 0.7 PV). The injected water could only be detected after averaging a couple of repeat CT-scans, and subtracting the average scan of the core with the original brine from the one with the NaI brine. Two characteristic cross sections are shown in Figure 1.

Here it can be seen that the core has a tortuous and complex network of very fine fractures; horizontal at one place, and vertical a few centimetres away. Some of these could just be seen on the initial scans, but certainly not all, let alone the connectivity. A 3D-image shows that there is a continuous path through the core, but no leakage along its surface or along the inside of the aluminium mantle.

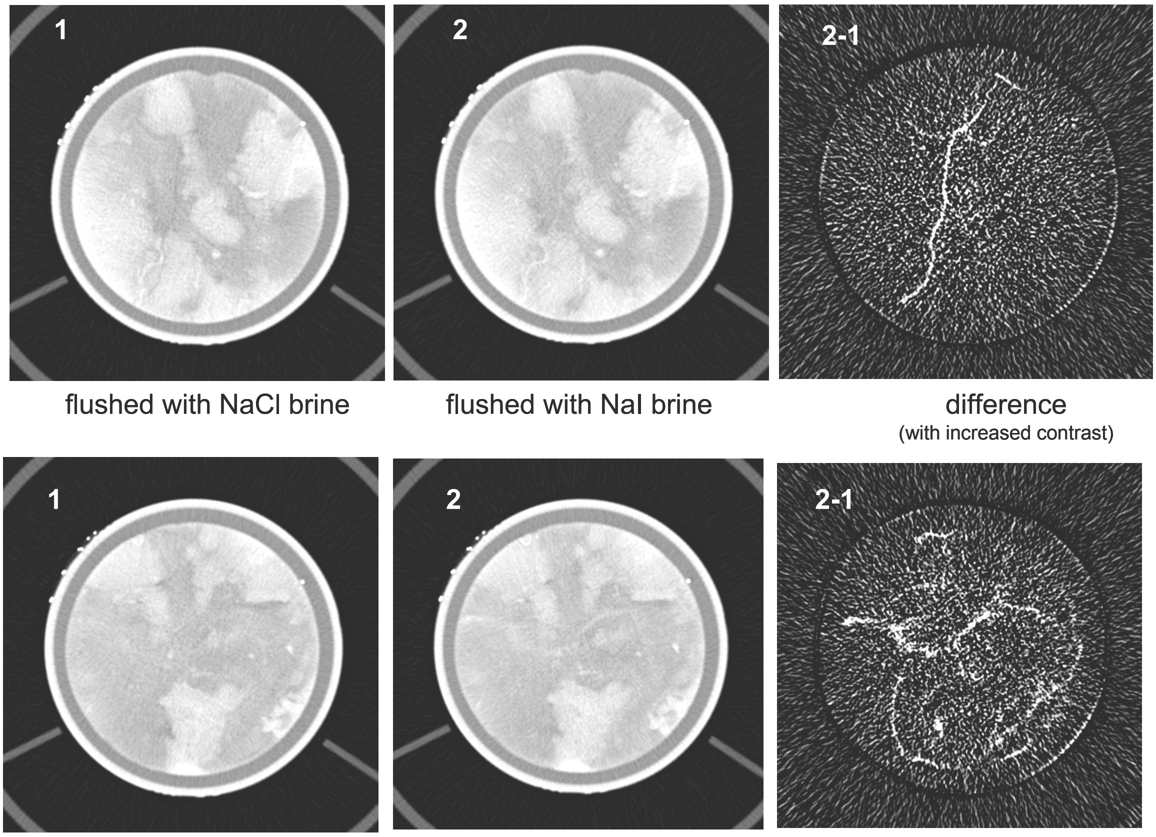

Figure 1. Two characteristic slices of Core-B after (early) water breakthrough. The water path is clearly visible on the difference picture where the water shows up due the large cross section of Iodine.

The pressure development over time shows a steady upward trend, while the flow rate was kept constant. After corrections for pressure drop in the flow lines and for a pressure offset, the water permeability was found to have decreased from 15 to 8 mD at the end of the flooding period. The NaI flood did not cause a change in the observed pressure trend.

The actual width of the fractures is less than seen on the scan due to the finite resolution of the inversion kernel. Our analysis of the scan resolution below indicates that the fracture has a typical aperture of 35 μm. This is consistent with the observed water permeability: using the approach given by Tiab and Donaldson, Chapter 8 [3], a single fracture of 25 μm wide in a core of 10 cm diameter results in an apparent permeability of 8 mD .

Mechanical causes

We analysed the possible mechanical forces on the core during the experiments. The thermal expansion of the materials (aluminium, resin and limestone) is not the same. In particular, aluminium has a greater thermal expansion coefficient than limestone. The maximum effect could increase the annulus between aluminium mantle and core by 23 µm when the temperature is raised by 20^{o}C. The effect due to shrinkage of the resin during curing is negligible for the resin used.

The above two effects, if fully transferred to strain in the elastic resin, would exert a pulling force on the outer surface of the core in the order of no more than hundred Newton. It is questionable if that would be enough to induce a completely new fracture, but it could be enough to enlarge an already present one. Similarly, it would result in a mildly confining stress when temperature is lowered.

The dilatation caused by temperature increase to 40^{o}C is comparable to the fracture width. However, as mentioned above, the corresponding force is not sufficient to break a competent rock, and initial onsets of fractures must have existed already.

Fracture width from CT scan

CT scanning is an ideal technique to visualise the presence of fractures inside a core, see for example [4]. However, the width of the fracture cannot be directly measured from the CT-scans when it is much less than the spatial resolution of the scans. The spatial resolution is determined by a combination of the pixel size and the inversion kernel. The pixel size depends on the field of view and the number of pixels. In our case the field of view was 130 mm and the number of pixels 512; hence one pixel is 0.26 mm wide (and high).

A CT image is the result of a back-calculation (inversion) of measurements of X-ray attenuation along a large number of lines through a slice of core. In the ideal case, the inversion precisely restores the original. In reality the result has a finite size. This is known as the inversion kernel, and forms a compromise between spatial sharpness and noise in the pixel value.

We analysed the cross sectional scan of a test tube partly filled with water, see Figure 2. The effect of the inversion kernel can be modeled by a smoothing filter operation. Knowing the true thickness of the test tube's glass wall allows us to determine the filter coefficients by minimizing the difference between a filtered version of the model and the measured response. The true CT value for the glass was also treated as an adjustable parameter; the value found agrees well with the bulk value for glass. Repeats made on different scans found the same filter values. It shows that the kernel that is normally used for 3D images (B45medium) averages over 4 pixels.

To test this interpretation, we placed a strip of aluminium foil in the test tube, see Figure 2. The foil was 30 µm thick, and the strip was oriented along the axis of the scanner similar as a fracture that runs along the length of a core. Because of the finite spatial resolution of the scan, the foil does not reach the true aluminum value, and is more than a pixel wide. The above inverse filter operation restores the true pixel reading, and finds a CT value that is still less than that of bulk aluminum. The pixel value, corrected for the water background, is 0.13 of the bulk aluminium value, which means that the foil thickness is only 0.13 times that of a pixel. This amounts to a thickness of 0.13 * 0.26 mm = 35 µm, which is indeed about the right value.

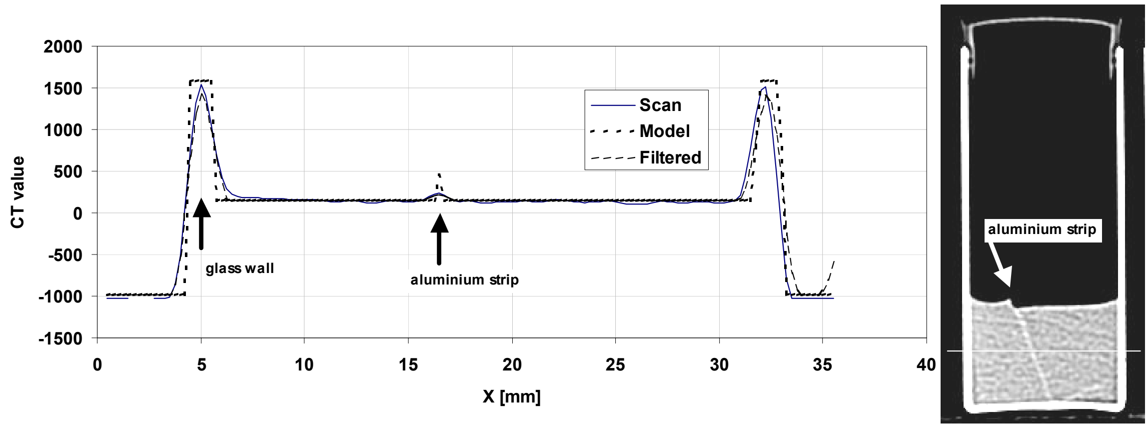

Figure 2. CT values of a test tube with brine and a thin aluminium strip (L-shaped). The data were taken along the horizontal line shown. The Model has the true pixel values, and the Filtered curve is a simulation of the measured Scan.

The above deconvolution technique (i.e. inverse filtering) was then applied to find the width of the fracture. An illustrative example is shown in Figure 3 taken across the fracture shown in Figure 1 (top). The inversion finds the height of the peak such that the filtered response matches the actually measured response. The bulk value of the NaI brine minus that of the NaCl brine amounts 4000 while zero is at -1000. Hence, the fracture width varies between 0.1 and 0.2 of the pixel size, i.e. 30 to 65 µm. From other scans we find similar values, generally in the range of up to ~100 µm when the fracture is clearly visible, but often less than 30 µm.

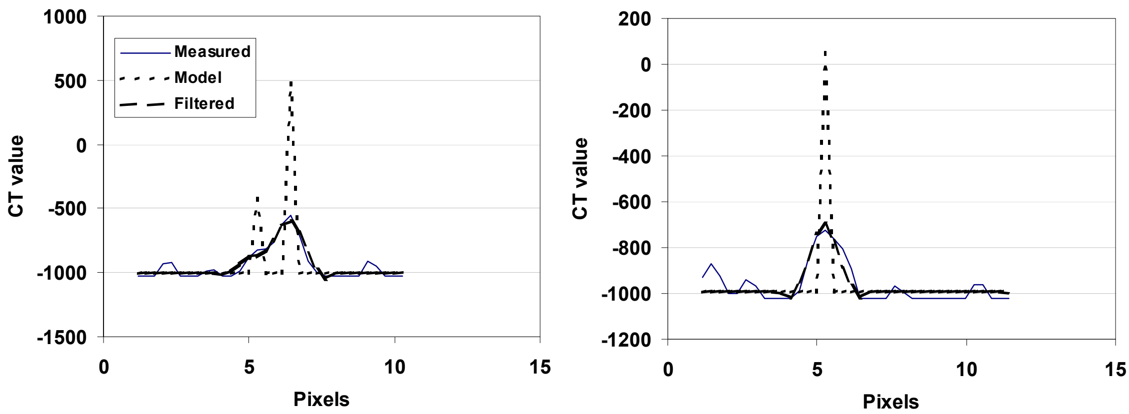

Figure 3. CT values across two positions of a fracture and interpreted model. The pixel size is 0.3 mm. The peaks in Model do not reach the full NaI-brine value, indicating that the fracture is less than one pixel wide.

Fracture size and path

Core-B was at initial water saturation when the waterflood started, and should thus have a very low (relative) permeability to water. The observed permeability and almost instantaneous water breakthrough can only be explained by a fracture through the core, or an annular leak. Inspection of the scans with and without NaI-brine flood rules out the latter, and shows that a fine, tortuous fracture network exists through the core. As mentioned, the fracture aperture, estimated from the scans, amounts to approximately 25 µm, which is consistent with the observed permeability of 8 to 15 mD.

The oil permeability of 47 mD is a combination of genuine matrix permeability and fracture permeability: the fracture is likely to have about the same permeability to either fluid (the aperture is too wide to see wettability effects). To first order matrix and fracture permeability can be treated as parallel conduits. With these assumptions, it then follows that the matrix permeability to oil is about 30 mD, which is not unrealistic. Since this is a larger conduit than the fracture, it explains that the core could be resaturated during the oil flood.

CONCLUSIONS

Although the results of the experiments could not provide the planned data to verify the numerical simulations, a number of significant insights have been obtained.

- Fractures even as small as ten micrometers wide make water flooding of an oilwet core to result in early water breakthrough without any significant oil production. The origin of the fracture is of secondary importance for this conclusion.
- Differential 3D scans of the core with NaI-doped brine and undoped brine, respectively, proved very powerful to visualize a network of fractures as narrow as a few tens of micrometers.
- A simple deconvolution scheme (inverse modeling) was used on CT images data to quantify the fracture width far less than the pixel size.
- Inspection of the fracture scan overlain on the normal scan does not show a preferred location for the fractures. At some locations it seems to follow the periphery of the nodules, at other places it cuts straight through matrix as well as nodules. There is no indication that rims have been water flooded, which means that the entry pressure of the higher permeable rims was not reached in these experiments.

ACKNOWLEDGEMENT

The authors like to thank many colleagues, in particular Issa Abu-Shiekah and Shehadeh Massalmeh, for valuable discussion and advice.

REFERENCES

1. Vinegar HJ, Wellington SL, Tomographic imaging of 3-phase flow experiments, Review Sci. Instr., (1987) 58, 96-107.
2. Fourar M, Konan G, Fichen C, Rosenberg E, Egermann P, and Lenormand R, 2005, Tracer tests for various carbonate cores using X-ray CT. SCA2005-56.
3. Tiab D and Donaldson EC, Petrophysics, 2nd edition, Elsevier, 2004, ISBN-13: 978-0-7506-7711-0.
4. Basquet R, Rennan L, Ringen JK and Wennberg OP, 2008, Fluid flow simulations on core samples containing natural fractures and styolites. SPE 113530.